Brain Imaging and Behavior (2011) 5:171–180
DOI 10.1007/s11682-011-9121-8

ORIGINAL RESEARCH

Diffusion Tensor Imaging in Huntington's disease reveals distinct patterns of white matter degeneration associated with motor and cognitive deficits

India Bohanna · Nellie Georgiou-Karistianis · Anusha Sritharan · Hamed Asadi · Leigh Johnston · Andrew Churchyard · Gary Egan

Published online: 26 March 2011

Abstract White matter (WM) degeneration is an important feature of Huntington's disease (HD) neuropathology. To investigate WM degeneration we used Diffusion Tensor Imaging and Tract-Based Spatial Statistics to compare Fractional Anisotropy, Mean Diffusivity (MD), parallel diffusivity and perpendicular diffusivity ($\lambda\perp$) in WM throughout the whole brain in 17 clinically diagnosed HD patients and 16 matched controls. Significant WM diffusivity abnormalities were identified primarily in the corpus callosum (CC) and external/extreme capsules in HD patients compared to controls. Significant correlations were observed between motor symptoms and MD in the CC body, and between global cognitive impairment and $\lambda\perp$ in the CC genu. Probabilistic tractography from these regions revealed degeneration of functionally relevant interhemispheric WM tracts. Our findings suggest that WM degeneration within interhemispheric pathways plays an important role in the deterioration of cognitive and motor function in HD patients, and that improved understanding of WM pathology early in the disease is required.

Keywords Huntington's disease · Diffusion tensor imaging · White matter · Tract-based spatial statistics · Corpus callosum

Abbreviations

HD	Huntington's disease
WM	White matter
DTI	Diffusion Tensor Imaging
TBSS	Tract-Based Spatial Statistics
FA	Fractional Anisotropy
$\lambda\perp$	Perpendicular diffusivity
$\lambda\|\|$	Parallel diffusivity
MD	Mean Diffusivity
ROI	Region-of-interest
UHDRS	Unified Huntington's Disease Rating Scale
MMSE	Mini Mental State Examination
BDI	Beck Depression Inventory
CAG	Cytosine-adenine-guanine
YSD	Years since diagnosis
NART	National Adult Reading Test
TR	Repetition time
TE	Echo time
FDT	FMRIBs Diffusion Toolbox

Electronic supplementary material The online version of this article (doi:10.1007/s11682-011-9121-8) contains supplementary material, which is available to authorized users.

I. Bohanna · H. Asadi · L. Johnston · G. Egan
Howard Florey Institute, Florey Neuroscience Institutes,
Parkville, Victoria, Australia

I. Bohanna · H. Asadi · G. Egan
Centre for Neuroscience, University of Melbourne,
Parkville, Victoria, Australia

N. Georgiou-Karistianis (✉) · A. Sritharan
Experimental Neuropsychology Research Unit,
School of Psychology and Psychiatry, Monash University,
Clayton, Victoria 3800, Australia
e-mail: nellie.georgiou-karistianis@med.monash.edu.au

L. Johnston
Department of Electrical and Electronic Engineering,
University of Melbourne,
Parkville, Victoria, Australia

A. Churchyard
Department of Neurology, Monash Medical Centre,
Clayton, Victoria, Australia

Introduction

Degeneration of striatal grey matter is the principal neuropathological feature of Huntington's disease (HD). Recently however, accumulating evidence suggests that white matter (WM) degeneration may also be important. Abnormalities in WM microstructure have been demonstrated in neuropathological studies of human HD (de la Monte et al. 1988; Mann et al. 1993; Sapp et al. 1999) as well as in animal models (Lee et al. 2004; Li et al. 1999; Wade et al. 2008) and Magnetic Resonance Imaging (MRI) studies reveal extensive WM volume loss (Aylward et al. 1998; Beglinger et al. 2005; Halliday et al. 1998; Paulsen et al. 2006; Rosas et al. 2003) and abnormal microstructure (Bartzokis et al. 2007; Fennema-Notestine et al. 2004; Jech et al. 2007; Kloppel et al. 2008; Mascalchi et al. 2004; Reading et al. 2005; Rosas et al. 2006; Stoffers et al. 2010). Examination of the relationship between WM structure and functional deficits suggests that WM degeneration plays an important role in functional decline, as evidenced by correlation of clinical symptom measures with those of WM volume (Beglinger et al. 2005; Halliday et al. 1998; Rosas et al. 2003), T1 signal intensity (Jech et al. 2007), and Diffusion Tensor Imaging (DTI) measures of microstructure (Kloppel et al. 2008; Rosas et al. 2006; Rosas et al. 2009).

DTI, which characterizes the diffusion of water in the brain, enables investigation of WM microstructure and identification of axonal tracts. Inferences about WM microstructure and pathological changes can be made using DTI measures such as Fractional Anisotropy (FA) (Basser & Pierpaoli 1996), which characterizes the anisotropy of the fiber structure, or the degree to which diffusivity is greater along some directions compared to others. FA is highest in highly organized WM tracts such as the corpus callosum (CC), where water diffusion in the direction parallel to axons is greater than in the perpendicular direction (Basser & Pierpaoli 1996). Mean diffusivity (MD), indicates the mean rate of diffusion, and is the equivalent of the mean of the eigenvalues. Analysis of directional diffusivities, parallel ($\lambda\|$) and perpendicular ($\lambda\perp$), may further clarify the underlying degenerative processes in WM in HD (Concha et al. 2006).

Studies of Wallerian degeneration in rodents and humans indicate that in WM, $\lambda\perp$ increases with demyelination (Concha et al. 2006; Glenn et al. 2003; Pierpaoli et al. 2001; Song et al. 2003; Sun et al. 2006), whilst $\lambda\|$ decreases during the acute phase of axonal degeneration as the axon fragments but may subsequently normalize or even increase (Concha et al. 2006; Song et al. 2003; Sun et al. 2006).

DTI studies in HD reported reduced anisotropy in the CC (Kloppel et al. 2008; Rosas et al. 2006; Rosas et al. 2009), internal and external/extreme capsules, in WM tracts associated with primarily frontal, motor, and sensory regions (Reading et al. 2005). In HD, DTI abnormalities in WM are also associated with reduced neuropsychological performance (Kloppel et al. 2008; Rosas et al. 2006; Rosas et al. 2009), and microstructural abnormalities appear to be progressive (Rosas et al. 2006; Stoffers et al. 2010; Weaver et al. 2009).

Voxelwise statistical analysis approaches can localize regional differences in WM microstructure, but may be sensitive to the effects of misregistration and spatial smoothing. Smith et al. (Smith et al. 2006) recently developed Tract Based Spatial Statistics (TBSS), which includes steps to minimize errors due to misregistration and smoothing. TBSS does not rely on perfect registration; a post-registration correction step finds the local WM tract center in each individual, thus accounting for residual registration error. Weaver et al. (Weaver et al. 2009) used TBSS and report longitudinal DTI changes after one year in 4 preclinical and 3 early clinical HD participants in subcortical, callosal and fronto-striatal WM, and suggest that DTI microstructure measures could serve as potential biomarkers for HD.

DTI tractography can be used to identify WM pathways and structural connections of interest. TBSS and tractography can be used in a complementary way to characterize the structural connectivity of the brain. In a study by Johansen-Berg et al. (Johansen-Berg et al. 2007), in healthy controls, TBSS revealed a region in the CC body where bimanual motor task performance and FA were significantly correlated. When used as an initiation point for tractography, tracts from this region connected bilateral premotor/supplementary motor cortical regions, highlighting the importance of these connections in bimanual motor function.

Our objective was to firstly map regional abnormalities in FA, MD, $\lambda\|$ and $\lambda\perp$ throughout the whole brain in HD patients using TBSS. We anticipated that a whole brain TBSS analysis would reveal the full extent of regional WM diffusivity abnormalities associated with HD, and that FA, MD, $\lambda\|$ and $\lambda\perp$ measures would further elucidate the contribution of axon and myelin pathology to WM abnormalities. In HD patients, we used TBSS to determine how variability in microstructure in the WM network correlated with motor symptoms, global cognitive impairment and psychiatric symptoms and used tractography to identify the WM pathways and cortical grey matter regions involved. We hypothesized that decline in motor, cognitive and psychiatric function would be associated with degenerative changes in WM microstructure and WM pathways, as revealed by tractography.

Methods

Participants

This study was approved by the ethics committees of the Howard Florey Institute and Monash University, and written informed consent was obtained. 20 genetically tested HD individuals and 18 healthy age-matched controls participated. Participants were excluded if movement artifacts were present on their T1 structural or DTI images, resulting in exclusion of three HD patients. Data for two control participants was excluded due to incomplete acquisition, with 17 HD patients and 16 control subjects included in the final analysis (Table 1). Based on the clinical judgment of the assessing neurologist, all HD participants were diagnosed as symptomatic (UHDRS motor score >5) (Tabrizi et al. 2009). Motor symptom severity was rated using the motor scale of the Unified Huntington's Disease Rating Scale (UHDRS) (Huntington Study (Group 1996)). HD patients continued their prescribed medication regimen during the study. Three patients were unmedicated, with the remaining taking one or more medications: antidepressants including paroxetine, fluvoxamine, sertraline, citalopram; antipsychotics including, haloperidol, olanzapine; and lithium as a mood stabilizer. Eight patients were taking neuroleptic medication and one was taking simvastatin to lower cholesterol. Pre-morbid IQ was assessed using the National Adult Reading Test (NART) (Nelson & Willison 1982) and global cognitive impairment was evaluated using the Mini Mental State Examination (MMSE) (Folstein et al. 1975). Participants also completed the Beck Depression Inventory (BDI) (Beck et al. 1961) to measure symptoms of depression.

Image acquisition and processing

Diffusion weighted images were obtained using a 3T scanner (General Electrics, Milwaukee, WI, USA) and double spin echo diffusion weighted EPI sequence (TR/TE=5800/82.3 milliseconds). Whole brain volumes were acquired with 50 contiguous axial slices (slice thickness=2.5 mm, acquisition matrix=128×128, field of view=24 cm^2, voxel size=1.875×1.875×2.5 mm). Diffusion-sensitizing encoding gradients were applied in 28 directions (b=1200s/mm^2) and five volumes without diffusion weighting (b=0s/mm^2) were also acquired. Structural T1 images were also obtained and used to estimate whole brain, grey and white matter volumes (TR/TE=500/15 milliseconds, acquisition matrix=512×512, field of view=25.6 cm^2, slice thickness=2.0 mm, voxel size =0.5×0.5×2.0 mm).

Analysis was performed using FSL 4.1. FAST to obtain grey and white matter volumes for each participant. FMRIBs Diffusion Toolbox (FDT) was used to correct for head movement and eddy and to generate FA, MD, $\lambda\|$ and $\lambda\perp$ images. TBSS was used for voxelwise analysis of FA, $\lambda\|$ and $\lambda\perp$ images. TBSS nonlinearly registered all participants' FA volumes to a standard template FA volume (an average of 58 aligned FA volumes). The success of registration of each participant's FA volume to the FA template was verified by visual inspection. Mean FA and skeletonized mean FA volumes were then generated (Fig. 1a), representing the center of major WM tracts throughout the whole brain (thresholded to exclude voxels with FA≤0.25). TBSS was able to accurately identify the WM tract center (Supplementary Fig. 1). The same registration and masking steps used for the FA data were then applied to the MD, $\lambda\|$ and $\lambda\perp$ maps.

Table 1 Demographic and clinical characteristics of control and HD groups

Characteristic	Control (n=16)	HD (n=17)	Sig.[c]
Mean age (years)	49.8 (range 38–59)	50.7 (range 37–64)	NS
Gender (m:f)	14:2	16:1	
Mean IQ[a]	115.7 (range 111–126)	114.4 (range 108–124)	NS
Mean Years of Education	14.0 (range 11–18)	13.1 (range 10–17)	NS
Mean MMSE	29.1 (range 26–30)	26.3 (range 20–30)	p=.004
Mean BDI	1.5 (range 0–5)	8.5 (range 0–32)	p=.01
Mean UHDRS motor	NA	28.7 (range 10–52)	
Mean YSD	NA	6.8 (range 2–13)	
Mean CAG repeat length[b]	NA	42.7 (range 36–46)	

MMSE Mini Mental State Examination; *BDI* Beck Depression Inventory; *UHDRS* Unified Huntington's Disease Rating Scale; *YSD* years since diagnosis; *CAG*, cytosine-adenine-guanine

[a] IQ, estimated full scale IQ calculated from National Adult Reading Test error score

[b] 2 participants did not contribute CAG repeat information, 1 participant had a CAG repeat of 36, all other participants had CAG repeat lengths ≥40

[c] Obtained by nonparametric Mann Whitney U test for independent samples. NS=Not significant at the p<.05 level

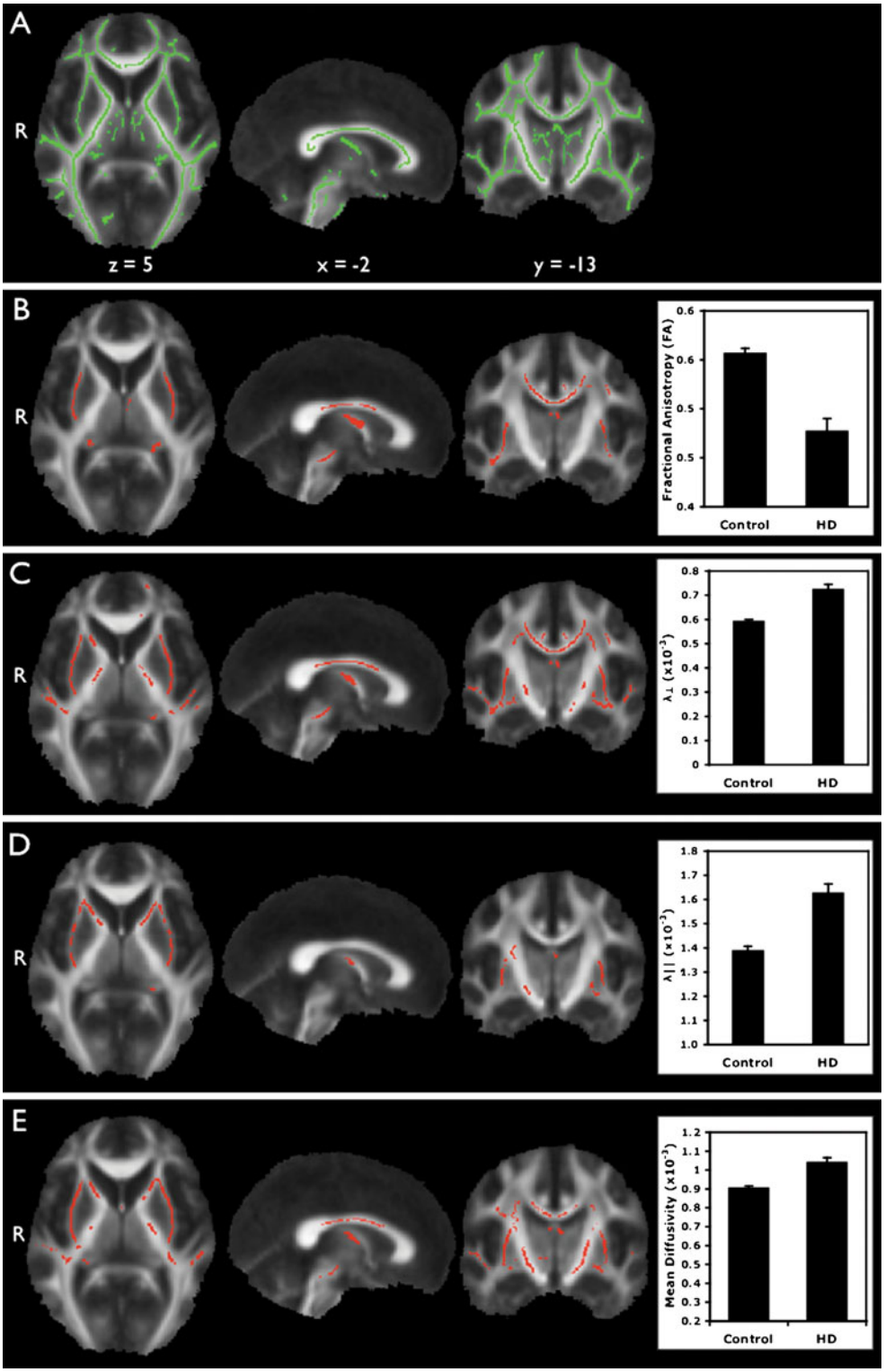

Fig. 1 **a** Mean FA image (grey-scale) overlaid with skeletonized mean FA image (*green*, thresholded at FA≥0.25), for the control and HD groups combined. Results of TBSS analysis between HD and control groups, showing regions (*red*) of significantly decreased **b** FA, and significantly increased **c** λ⊥, **d** λ|| and **e** MD in HD patients. Coordinates for (**b**–**e**) are the same as those listed in (**a**). Histograms show the mean and standard error of the mean for regions of significant difference between control and HD groups

Statistical analysis

Voxelwise statistical comparisons of skeletonized FA, MD, λ|| and λ⊥ were conducted using FSL-Randomise (Nichols & Holmes 2002), using a threshold *of* $p<.05$, corrected at cluster level for multiple comparisons. We used a cluster-forming threshold of $t>3$ to identify extended regions of significantly different DTI measures between HD and control participants. Randomise was also used to identify clusters of voxels where diffusivity measures were significantly correlated with UHDRS, BDI and MMSE scores, CAG and YSD *(*$p<.05$). Age

was included as a covariate of no interest. Correlation strengths were obtained within clusters showing significant correlations between diffusivity and clinical measures, with all correlations controlling for age.

Probabilistic tractography

The selection of initiation points used for tractography was based on clusters displaying the strongest voxelwise correlations with UHDRS and MMSE score. One ROI was located in the genu of the CC where $\lambda\perp$ correlated with MMSE, and a second ROI was located in the CC body where MD correlated with UHDRS motor score. To identify cortical connections from each ROI, we used masks of cortical regions identical to those previously used to map thalamic connections (Behrens et al. 2003), namely the prefrontal, premotor/supplementary motor, primary motor, primary/secondary somatosensory, posterior parietal, temporal and occipital cortices.

FDT was used to generate probabilistic tracts between the seed points and the cortical target masks (Behrens et al. 2003). Individual tracts were thresholded to include voxels with a value≥0.25% of the maximum connectivity value in the tract, to eliminate erroneous tracts while still preserving those with weak connectivity. Tract maps were binarized, nonlinearly registered to standard space, then combined to generate group tract maps. Group tract maps were thresholded to only include voxels present in the pathways of at least 47% (8/17) of patients, to identify pathways that were common among individuals while still allowing the variability among individuals to be represented. For each subject, the percentage of the total number of voxels in the seed ROI that showed supra-threshold connectivity to each cortical target was recorded.

Results

Brain volumes

HD patients had a total brain volume of 1,352±47 cm^3 (mean±SD), which was not significantly different from controls (1,370±29 cm^3). HD patients had significantly reduced ($p<.05$) grey matter volume (676±24 cm^3) compared to controls (707±14 cm^3), a difference of 4.5%. There was no significant difference ($p=0.41$) in WM volume between controls (662±16 cm^3) and HD patients (676±24 cm^3).

TBSS whole brain comparison of diffusion measures

Clusters of significantly ($p<.05$) altered FA, $\lambda\|$ and $\lambda\perp$ and MD in HD patients compared to controls are shown in Fig. 1. FA decreases and MD increases were significant in HD patients compared to controls in the CC (genu, body and splenium), fornix, external/extreme capsules, bilateral corona radiata (superior, anterior and posterior) and sagittal stratum. FA was significantly reduced additionally in the left posterior thalamic radiation and left superior longitudinal fasciculus (Fig. 1b), whilst MD was significantly increased also in the right superior longitudinal fasciculus, bilateral internal capsule (anterior and posterior) and bilateral cerebral peduncles (Fig. 1e). There were no areas of significantly increased FA or significantly reduced MD in HD patients compared to controls. $\lambda\perp$ was significantly ($p<.05$) increased in HD patients compared to controls in the CC (genu, body and splenium), fornix, external/extreme capsules, internal capsules (mainly posterior limbs), corona radiata (superior, anterior and posterior), sagittal striatum, cingulum, superior longitudinal fasciculi and in the left posterior thalamic radiation (Fig. 1c). $\lambda\|$ was significantly ($p<.05$) increased in HD patients in the corona radiata (superior, anterior and posterior), internal capsules (mainly anterior limbs), external/extreme capsules, fornix and left superior longitudinal fasciculus (Fig. 1d). There were no areas of significantly ($p<.05$) decreased $\lambda\perp$ or $\lambda\|$ in HD patients compared to controls.

Correlations and tractography

Voxelwise correlations between the diffusion and clinical data in HD patients revealed several regions where variability in function correlated significantly ($p<.05$) with variability in diffusion measures. To determine the anatomical location and correlation strengths, significant clusters were segmented, based on a WM tract atlas (Mori & Wakana 2005), into smaller anatomically defined ROIs. Correlation strengths and cluster sizes are given in Table 2.

UHDRS motor score correlated most strongly with MD in a cluster in the body of the CC (177 voxels; $r=.87$, $p<.001$; Fig. 2a). This cluster in the CC body overlapped with a smaller cluster where UHDRS and $\lambda\perp$ were correlated. Motor score did not correlate significantly with either FA or $\lambda\|$. In HD patients, tractography from this ROI revealed connections with bilateral premotor and supplementary motor cortices and few connections with other cortices (Fig. 2a). Connectivity profiling of this seed ROI in HD patients demonstrated connectivity primarily with bilateral sensory and motor cortices (Fig. 3a).

MMSE score was most strongly correlated with $\lambda\perp$ in the genu of the CC (607 voxels; $r=-.85$, $p<.001$; Fig. 2b). MMSE score also correlated significantly ($p<.05$) with MD, FA and $\lambda\perp$ in other regions of the CC and corona radiata, and with $\lambda\|$ in the corona radiata. No significant ($p<.05$) correlations were found between BDI score, CAG or YSD and any of the diffusivity measures. Tractography in HD

Table 2 Voxel clusters where white matter diffusion measures were significantly correlated with functional score in HD patients

	MD			FA			λ⊥			λ‖		
	R	Size	*p*	R	Size	*p*	R	Size	p	R	Size	*p*
UHDRS												
Corpus callosum												
Genu	.76	113	.001									
Body	.87	177	<.001				.75	124	<.001			
Corona radiata												
Superior												
L	.73	114	.001				.71	57	.001			
Posterior												
R	.77	211	.001									
Internal capsule												
Anterior												
L	.84	187	<.001									
Posterior												
R	.78	82	<.001									
L	.79	212	<.001									
MMSE												
Corpus callosum												
Genu	−.83	697	<.001	.82	159	<.001	−.86	607	<.001			
Body	−.85	113	<.001	.74	56	.001	−.77	165	<.001			
Splenium	−.85	104	<.001				−.75	30	.001			
Corona radiata												
Anterior												
R	−.77	330	<.001	.75	185	.001						
L	−.79	564	<.001				−.79	416	<.001	−.73	47	.001
Superior												
R	−.69	107	.003	.74	53	.001	−.71	97	.001			
L	−.72	50	.002				−.71	79	.001			
Internal capsule												
Anterior												
R	−.8	41	<.001									
L	−.7	10	.003									

MMSE Mini Mental State Examination; *UHDRS* Unified Huntington's Disease Rating Scale; *FA* Fractional Anisotropy; *MD* Mean Diffusivity; λ⊥, Perpendicular Diffusivity; λ‖, Parallel Diffusivity

patients from this ROI revealed strong connections with bilateral prefrontal cortices (Fig. 2b). Connectivity profiling of the seed ROI in HD patients revealed an almost exclusive prefrontal cortex connectivity pattern across subjects, with negligible connectivity to other cortices evident (Fig. 3b).

Discussion

WM degeneration is increasingly postulated as an important feature of HD neuropathology. Using a combined TBSS and tractography approach, which is novel in HD, we observed distinct patterns of CC degeneration associated with declining motor and cognitive function. Motor deficits were most strongly associated with increased MD in the CC body. Tractography revealed that this region contained interhemispheric connections between bilateral premotor and supplementary motor cortices. Conversely, cognitive deficits were best predicted by increased λ⊥ in the CC genu, where interhemispheric connections between bilateral prefrontal cortices were identified. Overall, both FA and MD group differences appeared to be driven by increased λ⊥ (Fig. 1).

The results of the current study are in line with previous research implicating CC degeneration in HD. Kloppel et al.

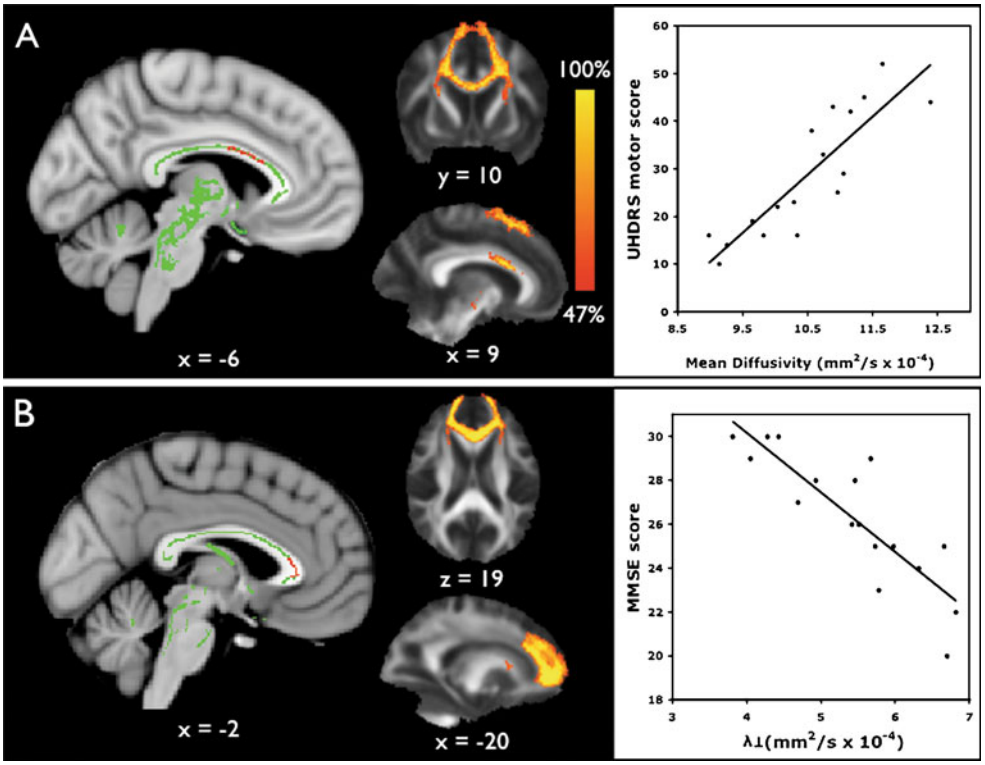

Fig. 2 Results of correlation in HD patients between **a** MD and UHDRS and **b** MMSE and λ⊥. The first images show the mean FA skeleton (*green*) overlaid with regions showing significant correlations (*red*). The central images show the connectivity distribution of tracts seeded from these ROIs. Scatterplots show mean ROI values plotted against the relevant score. Color scale/bar in tract image indicates voxels present in tracts of between 47% (8/17) and 100% (17/17) of HD patients. All correlations are partial correlations controlling for age

(Kloppel et al. 2008) showed that presymptomatic HD gene carriers could be differentiated from controls based on FA in the CC genu. CC microstructure has also been previously implicated in clinical symptoms. Rosas et al. (Rosas et al. 2006) demonstrated that FA in the CC correlated with performance on the Stroop colour word and verbal fluency tasks and more recently that CC λ⊥ also correlates with Symbol Digit and verbal fluency score (Rosas et al. 2009). The results we report here generally agree with those observed by Rosas et al. (Rosas et al. 2006) however we observed stronger correlations between motor and cognitive scores and the DTI measures, possibly due to the utilization of different approaches (ROI compared to voxelwise methods). In our study, neither CAG repeat length nor years since diagnosis correlated with the diffusivity measures. In pre-symptomatic HD gene carriers CAG repeat length and years to onset may be the best predictors of microstructural and morphological changes due to the reduced number of overt symptoms. However, the results of the present study suggest that clinical symptoms become more sensitive to tracking change in a symptomatic sample, possibly because the observable symptoms are more directly assessable. Furthermore, accumulating evidence suggests that in addition to abnormalities in cortico-striatal

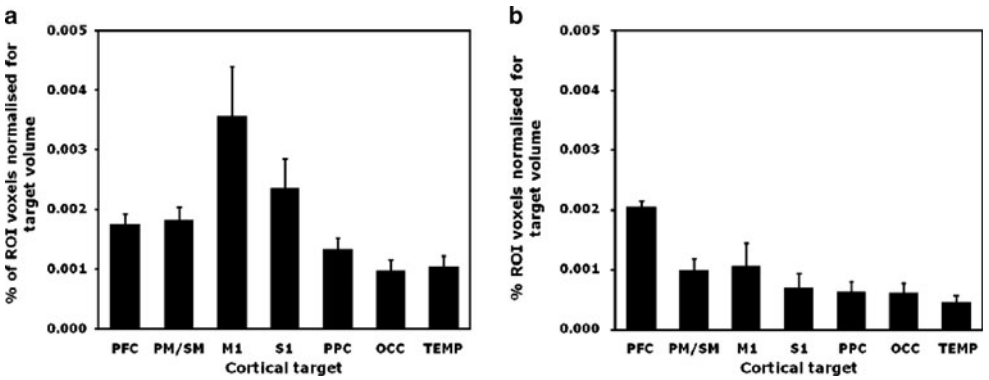

Fig. 3 **a** Connectivity profile of tractography seed ROI voxels where MD correlated with UHDRS score in the HD group, demonstrating that ROI voxels show connectivity primarily with sensorimotor cortical regions. **b** Connectivity profile of tractography seed ROI voxels where λ⊥ and MMSE were correlated in the HD group, demonstrating almost exclusive connectivity of the seed ROI with the prefrontal cortex. PFC, prefrontal cortex; PM/SM, premotor and supplementary motor cortex; PPC, posterior parietal cortex; M1, primary motor cortex; S1, somatosensory cortex; OCC, occipital cortex; TEMP, temporal cortex

pathways, interhemispheric connectivity also influences motor and cognitive function in HD.

Interhemispheric connectivity between sensory and motor cortices via the CC is crucial for coordinated movement, even though a breakdown in striatal outflow pathways is generally considered to precipitate motor deficits in HD. Similarly, intact interhemispheric connectivity mediated via prefrontal callosal regions appears to be an important determinant of cognitive function, with genu microstructure known to predict performance on tests of working memory, problem solving and visuomotor integration, functions in which bilateral cortical recruitment is important (Sullivan et al. 2008). Our observation that MD in sensorimotor callosal fiber bundles is the best predictor of UHDRS score is consistent with HD being a motor disorder, and moreover, with the deterioration of interhemispheric motor WM pathways being an important contributor to motor disability in HD. Among other cognitive functions, the MMSE assesses working memory, attention and executive function (Folstein et al. 1983), all of which require interhemispheric communication. Therefore the correlation we observed between genu $\lambda\perp$ and declining MMSE score is consistent with the degeneration of interhemispheric prefrontal connections being involved in cognitive decline in HD.

Degeneration of sensorimotor and prefrontal regions of the CC observed here in HD patients could be a consequence of previously reported cortical thinning (Rosas et al. 2005; Rosas et al. 2008), since regional degeneration in the cortex may be mirrored in the CC (Ota et al. 2006; Sydykova et al. 2007). Certainly, Rosas et al. (Rosas et al. 2008) recently reported that in HD the most significant cortical thinning occurs in sensory and motor cortical regions, and this cortical degeneration may thus contribute to degeneration in corresponding CC regions.

Our results suggest that in addition to FA and MD, examination of $\lambda\perp$ and $\lambda\|$ could provide further insight into the complex neuropathology of HD. For example, we did not observe decreased FA in the internal capsule, though both $\lambda\|$ and $\lambda\perp$ were significantly increased in this region, suggesting microstructural changes were indeed present. Interestingly, motor and cognitive decline in HD patients was generally associated with increased MD and $\lambda\perp$, suggesting that demyelination might contribute to the development of functional deficits. Evidence of myelin breakdown in HD includes increased tissue water and altered iron levels in white matter identified using in vivo imaging (Bartzokis et al. 2007; Bartzokis et al. 1999; Bartzokis & Tishler 2000). Studies in rodents demonstrate decreased $\lambda\|$ following axonal injury, whereas in contrast, we observed increased $\lambda\|$ in the internal and external/extreme capsules of HD patients. As demonstrated by Concha et al. (Concha et al. 2006), changes in $\lambda\|$ are likely time-dependent, decreasing during the acute phase of injury then subsequently normalizing or increasing, as axon fragments are cleared and water content increases. This may explain the significant increase in $\lambda\|$ we and others observed (Stoffers et al. 2010; Rosas et al. 2009), since HD is a chronically degenerative disease. Interestingly, Weaver et al. (Weaver et al. 2009) alternatively demonstrated significantly decreased $\lambda\|$ over time in a small sample of HD patients, indicating it is currently difficult to interpret such changes.

The pathology of HD is complex, involving axonal dysfunction and degeneration (Lee et al. 2004; Wade et al. 2008; Li et al. 2001), demyelination (Jech et al. 2007), and microglial abnormalities (Tai et al. 2007a; Tai et al. 2007b). These numerous pathological processes likely have compounding and interacting effects on water diffusion, thus limiting our ability to interpret DTI changes observed here. HD participants in this study had significantly decreased grey matter volume, but no significant change in WM volume. Divergent findings have been reported by previous studies of symptomatic HD patients with comparable age and UHDRS motor scores. There are two reports of minimal or no WM atrophy (Kassubek et al. 2004; Thieben et al. 2002), whereas others have reported significant WM atrophy (Rosas et al. 2003; Rosas et al. 2006; Tabrizi et al. 2009; Ciarmiello et al. 2006). The grey and white matter volumes for the control subjects in this study were comparable to previously reported volumes in controls of comparable age (Blatter et al. 1995). Our findings suggest that WM volume and diffusion measures appear to provide complementary information about WM degenerative changes in HD.

The limitations of this study deserve mention. The approach used in this study does not take into account the contribution of striatal or cortical grey matter changes, which have been previously documented in HD, to functional decline. Nevertheless, the strong correlations we observed between WM diffusivity measures and functional deficits suggest that WM degeneration is an important contributor to functional decline in HD. Also, the MMSE broadly assesses cognitive functions including, but not limited to, those that deteriorate in HD, such as executive function, attention and working memory, which involve multiple functional networks. Nevertheless, we observed a strong linear relationship between $\lambda\perp$ and MMSE changes, even with a range of less than 10 points on the MMSE, indicating that the approach used in this study is highly sensitive. Future studies should correlate more sensitive and specific tests to assess a range of cognitive/neuropsychological domains known to deteriorate in HD with diffusivity measures, particularly bearing in mind our growing understanding of pre-diagnosis deficits revealed by large-scale studies (Tabrizi et al. 2009; Paulsen

et al. 2008). Due to the number of participants, we were not able to investigate the effect of gender or medication status on WM measures, though these are certainly topics of importance in HD. Lastly, a potential limitation is the ability of TBSS to accurately identify the tract center in the presence of WM atrophy, which is known to have a significant effect on other voxelwise analysis approaches (Smith et al. 2006). This is certainly a current limitation of the technique and is an important issue that remains to be addressed.

DTI is an emerging method for probing abnormalities in WM microstructure and brain connectivity in HD (Bohanna et al. 2008), as well as assessing the influence of these changes on brain function. We used TBSS as an exploratory tool, the results of which informed a more detailed tractographic study of specific pathways of interest. This complementary approach, unique in the field of HD research allowed us to investigate WM microstructure and connectivity, and suggests that interhemispheric connectivity is an important aspect of HD pathophysiology.

Acknowledgements This study was funded by grant number 234247 from the National Health and Medical Research Council (Australia). We sincerely thank all participants for their time and effort. We also thank the Brain Research Institute (Austin Hospital) for the use of the 3T GE scanner. This study was carried out at School of Psychology, Psychiatry and Psychological Medicine, Monash University, Clayton, Victoria 3800, Australia. IB is supported by an Australian Rotary Health scholarship.

References

Aylward, E. H., Anderson, N. B., Bylsma, F. W., Wagster, M. V., Barta, P. E., Sherr, M., et al. (1998). Frontal lobe volume in patients with Huntington's disease. *Neurology, 50*(1), 252–8.

Bartzokis, G., & Tishler, T. A. (2000). MRI evaluation of basal ganglia ferritin iron and neurotoxicity in Alzheimer's and Huntingon's disease. *Cellular and Molecular Biology (Noisy-le-grand), 46*(4), 821–833.

Bartzokis, G., Cummings, J., Perlman, S., Hance, D. B., & Mintz, J. (1999). Increased basal ganglia iron levels in Huntington disease. *Archives of Neurology, 56*(5), 569–74.

Bartzokis, G., Lu, P. H., Tishler, T. A., Fong, S. M., Oluwadara, B., Finn, J. P., et al. (2007). Myelin breakdown and iron changes in Huntington's disease: pathogenesis and treatment implications. *Neurochemical Research, 32*(10), 1655–64.

Basser, P. J., & Pierpaoli, C. (1996). Microstructural and physiological features of tissues elucidated by quantitative-diffusion-tensor MRI. *Journal of Magnetic Resonance. Series B, 111*(3), 209–19.

Beck, A. T., Ward, C. H., Mendelson, M., Mock, J., & Erbaugh, J. (1961). An inventory for measuring depression. *Archives of General Psychiatry, 4*, 561–71.

Beglinger, L. J., Nopoulos, P. C., Jorge, R. E., Langbehn, D. R., Mikos, A. E., Moser, D. J., et al. (2005). White matter volume and cognitive dysfunction in early Huntington's disease. *Cognitive and Behavioral Neurology, 18*(2), 102–7.

Behrens, T. E. J., Johansen-Berg, H., Woolrich, M. W., Smith, S. M., Wheeler-Kingshott, C. A. M., Boulby, P. A., et al. (2003). Non-invasive mapping of connections between human thalamus and cortex using diffusion imaging. *Nature Neuroscience, 6*(7), 750–7.

Blatter, D., Bigler, E., Gale, S., Johnson, S., Anderson, C., Burnett, B., et al. (1995). Quantitative volumetric analysis of brain MR: normative database spanning 5 decades of life. *American Journal of Neuroradiology, 16*(2), 241.

Bohanna, I., Georgiou-Karistianis, N., Hannan, A. J., & Egan, G. F. (2008). Magnetic resonance imaging as an approach towards identifying neuropathological biomarkers for Huntington's disease. *Brain Research Reviews, 58*(1), 209–25.

Ciarmiello, A., Cannella, M., Lastoria, S., Simonelli, M., Frati, L., Rubinsztein, D. C., et al. (2006). Brain White-Matter Volume Loss and Glucose Hypometabolism Precede the Clinical Symptoms of Huntington's Disease, *Journal of Nuclear Medicine* (Vol. 47, pp. 215–222): Soc Nuclear Med.

Concha, L., Gross, D. W., Wheatley, B. M., & Beaulieu, C. (2006). Diffusion tensor imaging of time-dependent axonal and myelin degradation after corpus callosotomy in epilepsy patients. *Neuroimage, 32*(3), 1090–9.

de la Monte, S. M., Vonsattel, J. P., & Richardson, E. P., Jr. (1988). Morphometric demonstration of atrophic changes in the cerebral cortex, white matter, and neostriatum in Huntington's disease. *Journal of Neuropathology and Experimental Neurology, 47*(5), 516–25.

Fennema-Notestine, C., Archibald, S. L., Jacobson, M. W., Corey-Bloom, J., Paulsen, J. S., Peavy, G. M., et al. (2004). In vivo evidence of cerebellar atrophy and cerebral white matter loss in Huntington disease. *Neurology, 63*(6), 989–95.

Folstein, M. F., Folstein, S. E., & McHugh, P. R. (1975). Mini-mental state. A practical method for grading the cognitive state of patients for the clinician. *Journal of Psychiatric Research, 12*(3), 189–98.

Folstein, M. F., Robins, L. N., & Helzer, J. E. (1983). The mini-mental state examination. *Archives of General Psychiatry, 40*(7), 812.

Glenn, O. A., Henry, R. G., Berman, J. I., Chang, P. C., Miller, S. P., Vigneron, D. B., et al. (2003). DTI-based three-dimensional tractography detects differences in the pyramidal tracts of infants and children with congenital hemiparesis. *Journal of Magnetic Resonance Imaging, 18*(6), 641–8.

Group, H. S. (1996). Unified Huntington's disease rating scale: reliability and consistency. Huntington study group. *Movement Disorders, 11*(2), 136–42.

Halliday, G. M., McRitchie, D. A., Macdonald, V., Double, K. L., Trent, R. J., & McCusker, E. (1998). Regional specificity of brain atrophy in Huntington's disease. *Experimental Neurology, 154*(2), 663–72.

Jech, R., Klempir, J., Vymazal, J., Zidovska, J., Klempirova, O., Ruzicka, E., et al. (2007). Variation of selective gray and white matter atrophy in Huntington's disease. *Movement Disorders, 22*(12), 1783–9.

Johansen-Berg, H., Della-Maggiore, V., Behrens, T. E. J., Smith, S. M., & Paus, T. (2007). Integrity of white matter in the corpus callosum correlates with bimanual co-ordination skills. *Neuroimage, 36*, 16–21.

Kassubek, J., Bernhard Landwehrmeyer, G., Ecker, D., Juengling, F., Muche, R., Schuller, S., et al. (2004). Global cerebral atrophy in early stages of Huntington's disease: quantitative MRI study. *NeuroReport, 15*(2), 363.

Kloppel, S., Draganski, B., Golding, C. V., Chu, C., Nagy, Z., Cook, P. A., et al. (2008). White matter connections reflect changes in voluntary-guided saccades in pre-symptomatic Huntington's disease. *Brain, 131*(Pt 1), 196–204.

Lee, W. C. M., Yoshihara, M., & Littleton, J. T. (2004). Cytoplasmic aggregates trap polyglutamine-containing proteins and block axonal transport in a Drosophila model of Huntington's disease.

Proceedings of the National Academy of Science, 101(9), 3224–9.

Li, H., Li, S. H., Cheng, A. L., Mangiarini, L., Bates, G. P., & Li, X. J. (1999). Ultrastructural localization and progressive formation of neuropil aggregates in Huntington's disease transgenic mice. *Human Molecular Genetics, 8*(7), 1227–36.

Li, H., Li, S. H., Yu, Z. X., Shelbourne, P., & Li, X. J. (2001). Huntingtin aggregate-associated axonal degeneration is an early pathological event in Huntington's disease mice. *The Journal of Neuroscience, 21*(21), 8473.

Mann, D. M., Oliver, R., & Snowden, J. S. (1993). The topographic distribution of brain atrophy in Huntington's disease and progressive supranuclear palsy. *Acta Neuropathologica, 85*(5), 553–9.

Mascalchi, M., Lolli, F., Della Nave, R., Tessa, C., Petralli, R., Gavazzi, C., et al. (2004). Huntington disease: volumetric, diffusion-weighted, and magnetization transfer MR imaging of brain. *Radiology, 232*(3), 867–73.

Mori, S., & Wakana, S. (2005). MRI atlas of human white matter.

Nelson, H. E., & Willison, J. (1982). *National adult reading test (NART): Test manual*. Windsor: Nfer-Nelson.

Nichols, T. E., & Holmes, A. P. (2002). Nonparametric permutation tests for functional neuroimaging: a primer with examples. *Human Brain Mapping, 15*(1), 1–25.

Ota, M., Sato, N., Ohya, Y., Aoki, Y., Mizukami, K., Mori, T., et al. (2006). Relationship between diffusion tensor imaging and brain morphology in patients with myotonic dystrophy. *Neuroscience Letters, 407*(3), 234–9.

Paulsen, J. S., Magnotta, V. A., Mikos, A. E., Paulson, H. L., Penziner, E., Andreasen, N. C., et al. (2006). Brain structure in preclinical Huntington's disease. *Biological Psychiatry, 59*(1), 57–63.

Paulsen, J. S., Langbehn, D. R., Stout, J. C., Aylward, E., Ross, C. A., Nance, M., et al. (2008). Detection of Huntington's disease decades before diagnosis: the Predict-HD study. *Journal of Neurology, Neurosurgery and Psychiatry, 79*(8), 874–80.

Pierpaoli, C., Barnett, A., Pajevic, S., Chen, R., Penix, L. R., Virta, A., et al. (2001). Water diffusion changes in Wallerian degeneration and their dependence on white matter architecture. *Neuroimage, 13*(6 Pt 1), 1174–85.

Reading, S. A., Yassa, M. A., Bakker, A., Dziorny, A. C., Gourley, L. M., Yallapragada, V., et al. (2005). Regional white matter change in pre-symptomatic Huntington's disease: a diffusion tensor imaging study. *Psychiatry Research, 140*(1), 55–62.

Rosas, H. D., Koroshetz, W. J., Chen, Y. I., Skeuse, C., Vangel, M., Cudkowicz, M. E., et al. (2003). Evidence for more widespread cerebral pathology in early HD: an MRI-based morphometric analysis. *Neurology, 60*(10), 1615–20.

Rosas, H. D., Hevelone, N. D., Zaleta, A. K., Greve, D. N., Salat, D. H., & Fischl, B. (2005). Regional cortical thinning in preclinical Huntington disease and its relationship to cognition. *Neurology, 65*(5), 745–7.

Rosas, H. D., Tuch, D. S., Hevelone, N. D., Zaleta, A. K., Vangel, M., Hersch, S. M., et al. (2006). Diffusion tensor imaging in presymptomatic and early Huntington's disease: Selective white matter pathology and its relationship to clinical measures. *Movement Disorders, 21*(9), 1317–25.

Rosas, H. D., Salat, D. H., Lee, S. Y., Zaleta, A. K., Pappu, V., Fischl, B., et al. (2008). Cerebral cortex and the clinical expression of Huntington's disease: complexity and heterogeneity. *Brain, 131* (Pt 4), 1057–68.

Rosas, H. D., Lee, S. Y., Bender, A. C., Zaleta, A. K., Vangel, M., Yu, P., et al. (2009). Altered white matter microstructure in the corpus callosum in Huntington's disease: implications for cortical "disconnection". *Neuroimage, 49*(4), 2995–3004.

Sapp, E., Penney, J., Young, A., Aronin, N., Vonsattel, J. P., & DiFiglia, M. (1999). Axonal transport of N-terminal huntingtin suggests early pathology of corticostriatal projections in Huntington disease. *Journal of Neuropathology and Experimental Neurology, 58*(2), 165–73.

Smith, S. M., Jenkinson, M., Johansen-Berg, H., Rueckert, D., Nichols, T. E., Mackay, C. E., et al. (2006). Tract-based spatial statistics: voxelwise analysis of multi-subject diffusion data. *Neuroimage, 31*(4), 1487–505.

Song, S. K., Sun, S. W., Ju, W. K., Lin, S. J., Cross, A. H., & Neufeld, A. H. (2003). Diffusion tensor imaging detects and differentiates axon and myelin degeneration in mouse optic nerve after retinal ischemia. *Neuroimage, 20*(3), 1714–22.

Stoffers, D., Sheldon, S., Kuperman, J. M., Goldstein, J., Corey-Bloom, J., & Aron, A. R. (2010). Contrasting gray and white matter changes in preclinical Huntington disease: an MRI study. *Neurology, 74*(15), 1208–16.

Sullivan, E. V., Rohlfing, T., & Pfefferbaum, A. (2008). Quantitative fiber tracking of lateral and interhemispheric white matter systems in normal aging: relations to timed performance. *Neurobiology of Aging*

Sun, S. W., Liang, H. F., Le, T. Q., Armstrong, R. C., Cross, A. H., & Song, S. K. (2006). Differential sensitivity of in vivo and ex vivo diffusion tensor imaging to evolving optic nerve injury in mice with retinal ischemia. *Neuroimage, 32*(3), 1195–204.

Sydykova, D., Stahl, R., Dietrich, O., Ewers, M., Reiser, M. F., Schoenberg, S. O., et al. (2007). Fiber connections between the cerebral cortex and the corpus callosum in Alzheimer's disease: a diffusion tensor imaging and voxel-based morphometry study. *Cerebral Cortex, 17*(10), 2276.

Tabrizi, S. J., Langbehn, D. R., Leavitt, B. R., Roos, R. A., Durr, A., Craufurd, D., et al. (2009). Biological and clinical manifestations of Huntington's disease in the longitudinal TRACK-HD study: cross-sectional analysis of baseline data. *Lancet Neurol*.

Tai, Y. F., Pavese, N., Gerhard, A., Tabrizi, S. J., Barker, R. A., Brooks, D. J., et al. (2007a). Imaging microglial activation in Huntington's disease. *Brain Research Bulletin, 72*(2–3), 148–51.

Tai, Y. F., Pavese, N., Gerhard, A., Tabrizi, S. J., Barker, R. A., Brooks, D. J., et al. (2007b). Microglial activation in presymptomatic Huntington's disease gene carriers. *Brain, 130*(7), 1759.

Thieben, M. J., Duggins, A. J., Good, C. D., Gomes, L., Mahant, N., Richards, F., et al. (2002). The distribution of structural neuropathology in pre-clinical Huntington's disease. *Brain, 125* (8), 1815.

Wade, A., Jacobs, P., & Morton, A. J. (2008). Atrophy and degeneration in sciatic nerve of presymptomatic mice carrying the Huntington's disease mutation. *Brain Research, 1188*, 61–8.

Weaver, K. E., Richards, T. L., Liang, O., Laurino, M. Y., Samii, A., & Aylward, E. H. (2009). Longitudinal diffusion tensor imaging in Huntington's Disease. *Experimental Neurology, 216*(2), 525–9.